Published in final edited form as:
Biomaterials. 2013 January ; 34(1): 140–149. doi:10.1016/j.biomaterials.2012.09.045.

The role of endothelial cells in myofiber differentiation and the vascularization and innervation of bioengineered muscle tissue *in vivo*

Tracy L. Criswell[a], **Benjamin T. Corona**[b], **Zhan Wang**[a], **Yu Zhou**[a], **Guoguang Niu**[a], **Yong Xu**[c], **George J. Christ**[a], and **Shay Soker**[a,*]

Shay Soker: ssoker@wakehealth.edu

[a]Wake Forest Institute for Regenerative Medicine, Wake Forest University School of Medicine, Medical Center Boulevard, Winston-Salem, NC 27157, USA

[b]Extremity Trauma and Regenerative Medicine Research Program, United States Army Institute of Surgical Research, Fort Sam Houston, Texas, USA

[c]Department of Electrical and Computer Engineering, Virginia Tech, Blacksburg, VA 24061, USA

Abstract

Musculoskeletal disorders are a major cause of disability and effective treatments are currently lacking. Tissue engineering affords the possibility of new therapies utilizing cells and biomaterials for the recovery of muscle volume and function. A major consideration in skeletal muscle engineering is the integration of a functional vasculature within the regenerating tissue. In this study we employed fluorescent cell labels to track the location and differentiation of co-cultured cells *in vivo* and *in vitro*. We first utilized a co-culture of fluorescently labeled endothelial cells (ECs) and muscle progenitor cells (MPCs) to investigate the ability of ECs to enhance muscle tissue formation and vascularization in an *in vivo* model of bioengineered muscle. Scaffolds that had been seeded with both MPCs and ECs showed significantly greater vascularization, tissue formation and enhanced innervation as compared to scaffolds seeded with MPCs alone. Subsequently, we performed *in vitro* experiments using a 3-cell type system (ECs, MPCs, and pericytes (PCs)) to demonstrate the utility of fluorescent cell labeling for monitoring cell growth and differentiation. The growth and differentiation of individual cell types was determined using live cell fluorescent microscopy demonstrating the utility of fluorescent labels to monitor tissue organization in real time.

Keywords

Angiogenesis; Skeletal muscle; Tissue engineering; Progenitor cells; Fluorescent labeling

*Corresponding author. Tel.: +1 336 713 1325; fax: +1 336 713 7290.

Appendix A. Supplementary data: Supplementary data related to this article can be found at http://dx.doi.org/10.1016/j.biomaterials.2012.09.045.

1. Introduction

Musculoskeletal disorders are one of the most commonly diagnosed debilitating disorders in the United States. Current therapies are insufficient, often resulting in incomplete restoration of motility. Regenerative medicine and tissue engineering (TE) approaches have the potential to offer new possibilities for treatment. The ability to create large muscle tissue, that can be used to either enhance endogenous regeneration or to replace damaged tissue, would be therapeutically beneficial and have a major impact on increasing the quality of life for patients suffering from many musculoskeletal diseases and injuries.

TE is a highly dynamic process involving the single or combinatorial use of cells, scaffolds and factors that encourage cell growth and differentiation [1,2]. The ability to create a microenvironment, that can sustain the viability of cells and provide the appropriate matrix for differentiation and maturation, will be vital for successful tissue regeneration. Currently, TE of the cardiovascular system has had the most success in integrating these components and further applying them in a clinical setting [3,4]. TE of skeletal muscle is a complex process that requires myofiber formation, a coordinated construction of functional vasculature, innervation and the development of an extra-cellular environment that will allow for proper mechanical force production. Over the past decade, several studies have examined the role of each of these components in skeletal muscle TE [5–7], but few efforts have been made to examine and integrate all aspects required for the regeneration of functional muscle tissue.

We have previously demonstrated that neovascularization in engineered muscle tissues was enhanced when ECs and MPCs were injected into the subcutaneous space of mice [8]. We further demonstrated that VEGF secretion from MPCs during muscle tissue regeneration resulted in enhanced neovascularization and tissue volume preservation [9]. In addition, Saik *et al*., have shown that the addition of 10T1/2 cells as pericytes (PCs) to the culture of MPCs and ECs can result in the stabilization of bioengineered vessels [10]. In the current study, we utilized fluorescently labeled vascular cells, in combination with MPCs, to form new vessels concurrently with regenerating skeletal muscle on a biomaterial scaffold *in vivo*. Subsequently, we used fluorescent imaging to monitor tissue organization, non-invasively, in real time.

2. Methods

2.1. Antibodies and reagents

Recombinant human VEGF and heparin were purchased from R&D Systems (Minneapolis, MN). Matrigel was purchased from BD Biosciences (San Jose, CA). Qtracker 705 and CM-DiI were obtained from Invitrogen (Carlsbad, CA). Table 1 summarizes the primary and secondary antibodies used and dilutions. All biotinylated secondary antibodies were obtained from Vector Labs (Burlingame, CA).

2.2. Cell culture

2.2.1. MPC, EC, PC isolation and culture—Green fluorescent protein (GFP)-labeled muscle progenitor cells (GFP^+ MPCs) were derived from single muscle fibers isolated from

GFP-expressing mice (FVB.Cg-Tg(CAG-EGFP), Jackson Laboratory as previously described [11]. Briefly, muscle tissue was removed by micro-dissection, minced and digested in type I collagenase. Digested muscle tissue was plated on matrigel (BD Biosciences) coated six-well tissue culture plates containing DMEM (Hyclone, Thermo Scientific, Logan, UT) supplemented with 10% horse serum, 1% penicillin/streptomycin and 0.5% chick embryo extract (Hyclone) at 37°C in 5% CO_2 for 4–6 days. Isolated MPCs were trypsinized and grown in growth media (GM - DMEM containing 10% fetal bovine serum (FBS) and 1% penicillin/streptomycin) until use. MPCs were used no later than passage 2.

Human umbilical vein endothelial cells (HUVECs e ECs) were derived from human umbilical cords sourced from the Forsyth Medical Center in Winston-Salem with ethical approval and informed written consent as previously described [12], under the guidelines of our Institutional Review Board Committee approval. ECs were cultured on fibronectin (Millipore, Billerica, MA) coated plates in Endothelial Growth Medium 2 (EGM2, Lonza Biologics, Allendale, NJ) supplied with 10% FBS at 37°C in 5% CO^2. Cells were used no later than passage 5.

10T1/2 cells were used as our source of PCs and were a kind gift from Dr. Linda Metheney-Barlow (Wake Forest Baptist Health, Winston-Salem, NC). PCs were grown in DMEM containing 10% FBS at 37°C in 5% CO_2.

2.2.2. Cell labeling—ECs were labeled with CM-DiI (Invitrogen) and PCs were labeled with Qtracker 705 (Invitrogen) as per the manufacturers directions. Cells were used immediately after labeling and fluorescence was confirmed by microscopy. Cultures appearing to contain less than 95% labeled cells were discarded.

2.2.3. BAM and matrigel experimental procedures—Matrigel experiments were carried out in 4-well tissue culture chamber slides coated with a 1:5 dilution of matrigel. Bladder acellular matrix (BAM) scaffolds were derived from porcine bladder as previously described [13]. After decellularization, scaffolds were trimmed to a size of 2 × 3 cm and a thickness of 300–400 microns. Scanning electron microscopy (Hitachi Model S2260N) was performed to demonstrate collagen fiber morphology and arrangement as described [13].

Scaffolds were rehydrated in growth media (GM, DMEM + 10% FBS) 24 h prior to cell seeding. Approximately 8×10^5 total cells, in a 1:1:0.3 ratio of MPCs, ECs and PCs respectively were seeded on the BAM scaffold. Fewer numbers of PCs were used in the co-culture experiments, due to the very short doubling time of these cells, in order to prevent the over-growth of the PCs during the time course of the experiment. Scaffolds with MPCs alone had half as many cells as the co-cultured scaffolds. Seeded scaffolds were cultured for 3 days in GM at which point the medium was replaced with differentiation media (DMEM + 2% horse serum). Scaffolds were left in differentiation media (DM) for 4 days and then either implanted into nude mice (*in vivo* experiments) or placed back in GM (*in vitro* experiments) until end of experiment for *in vitro* procedures. For VEGF *in vitro* experiments, scaffolds were treated with either 10 U/ml heparin and/or 50 ng/μl VEGF. Supplemented media (either GM or DM) was replaced every 48 h.

2.3. Animal studies

All animal studies were performed in strict compliance with Wake Forest University IACUC and NIH guidelines. All experiments were performed on 8-week old female nude mice under anesthesia. A longitudinal excision was made along the mid-dorsal region of the back. Scaffolds were folded lengthwise, with cells exposed on either side, and inserted into the subcutaneous space adjacent to the incision. The incision was closed using simple interrupted 4-0 vicryl sutures. Scaffolds were excised at approximately 8 weeks and the dermis and subcutaneous adipose tissue were carefully removed from the scaffolds before being processed for histological evaluation.

2.4. Histology and immunohistochemistry

2.4.1. Histology—Scaffolds were explanted after 8 weeks, fixed in 10% neutral buffered formalin for 24 h and embedded in paraffin. Serial paraffin sections (8 mm) were analyzed using hematoxylin and eosin (H&E) staining for morphology and Masson's Tri-chrome stain to examine tissue formation and collagen deposition.

2.4.2. Immunohistochemistry—Antibodies used for tissue analyses are detailed in Table 1. Staining with monoclonal antibodies (mouse secondary) was performed using the M.O.M kit from Vector labs (Burlingame, CA). All other immunohistochemistry (IHC) procedures were performed as previously described [14]. Positive staining was visualized using the ImmPACT DAB Peroxidase kit from Vector Labs (Burlingame, CA) and counter-staining with Gill's heamatoxylin (Sigma Aldrich, St. Louis, MO). Images were captured using a Leica DM400B upright fluorescent microscope and a Retiga-2000RV Qimaging camera. Confocal images (Fig. 7) were acquired using Zeiss LSM 510 confocal microscope (Wake Forest Baptist Health Imaging Core). Real time *in vitro* imaging was captured using a Leica inverted fluorescent microscope, model DMI54000B with a QImaging Retiga-2000RV camera (Figs. 7 and 8).

2.4.3. Quantitation of in vivo data—Quantitation of vessels and tissue was performed using Trichrome stained sections. All quantitative experiments were performed on at least 5 scaffolds per experimental condition and were quantitated using ImageJ software. Blood vessel quantitation was performed by counting the number of vessels present on the scaffolds and expressed as number of vessels per high-powered field (HPFs). For tissue quantitation, scaffolds were sectioned entirely and every 10th slide was Tri-chrome stained and analyzed. Tissue area was outlined and then expressed as number of pixels per HPF. Innervation of the scaffolds was determined by counting the number of βIII tubulin$^+$ nerve bundles and expressed as number of bundles per HPF. Quantitating the number of DiI$^+$ (red) pixels per HPF was used to extrapolate the number of ECs on the scaffolds. Vessels were counted as branching structures with at least one intersecting point.

3. Results

3.1. Neovascularization of engineered muscle tissue

A major limitation in evaluating the cellular basis and mechanisms responsible for tissue formation using current TE technologies is the inability to monitor cell fate *in vivo*, which

requires long-lived labels. For the current research, we used muscle progenitor cells (MPCs) derived from the green fluorescent protein (GFP)-expressing mice and endothelial cells (ECs) that were labeled with CM-DiI (Supplemental Fig. 1). Scaffolds seeded with different combinations of MPCs and ECs were implanted in the mid-dorsal subcutaneous space of nude mice for approximately 8 weeks (Fig. 1A). Due to the poorly vascularized nature of the subcutaneous space, vascularization of the scaffold, either through infiltration of host vasculature or the stimulation of neovascularization from the use of angiogenic growth factors or ECs, would be required for any substantial tissue growth. In agreement with this, empty scaffolds that had not been seeded with cells, showed no vasculature infiltration or muscle tissue formation (Supplemental Fig. 2). Macroscopic observation of the explanted cell seeded scaffolds prior to fixation revealed a visible vascular network (data not shown), and vessels were observed infiltrating throughout the scaffold after fixation using bright field microscopy (Fig. 1B). The observation of GFP and DiI fluorescence indicated the presence of GFP^+ MPCs and CM-Dil-labeled ECs throughout the scaffold (Fig. 1C,D). The elongation and alignment of the GFP^+ MPCs within the scaffold suggest differentiation of these cells into myofibers (Fig. 1C, arrow) while the ECs appear to be aligned with blood vessels (Fig. 1D, arrow).

Trichrome stained sections of the explanted tissue revealed infiltration of blood vessels throughout the scaffold (Fig. 2A, arrows). Immunostaining for the pericyte marker CD146 showed localization of pericytes around the periphery of the vessels, suggesting that the vessels were mature and not under-developed nascent capillaries (Fig. 2B). We further utilized fluorescent microscopy to identify the location and differentiation status of the labeled cells. Several DiI-labeled ECs were observed integrated in the vasculature in the engineered tissue. These vessels were most likely functional since we were able to observe red auto-fluorescence generated by the erythrocytes within the vessels (Fig. 2C). It is interesting to note that no vessels were found entirely composed of implanted DiI-labeled ECs. IHC using an antibody specific to human CD31, which does not cross-react with the mouse CD31 antigen (Fig. 2D, inset), provided further confirmation that the ECs that were originally implanted with the engineered tissue, were present in the bioengineered muscle tissue (Fig. 2D, arrows). Further quantitative analysis showed a significant increase (more that 2-fold) in the number of vessels in the tissues that were engineered using a combination of ECs and MPCs, compared to tissues engineered with MPCs alone (Fig. 2E).

3.2. Myofiber formation in vivo

We subsequently examined the effect of ECs on MPC differentiation in the engineered muscle tissue *in vivo*. Specimens explanted 8 weeks after implantation revealed myofibers throughout the scaffold, as demonstrated by H + E and trichrome stains (Fig. 3A,B). TE muscle constructs demonstrated a heterogeneous morphology, in which a mixture of aligned and misaligned fibers (Fig. 3A, dashed area) are discernible within the scaffold (Fig. 3A, arrow), in addition to an assortment of fully mature striated muscle fibers (Fig. 3B, arrow) and immature fibers (Fig. 3B, arrowhead), as determined by the presence of centrally (immature) or peripherally (mature) located nuclei, respectively [15]. This observation indicated ongoing myo-differentiation and tissue growth, which is suggestive of myofiber self-renewal in the engineered tissue. All of the myo-fibers within the explanted engineered

muscles expressed GFP, indicating their origination from the implanted MPCs (Fig. 3C). GFP expression was further confirmed by immunohistochemistry using an antibody against GFP protein (Fig. 3D).

The myogenic differentiation of implanted MPCs was not dependent on the presence of ECs, as myofibers were found under both single and co-cultured experimental conditions. Trichrome stain analyses showed a close association, and integration, of blood vessels within the engineered muscle tissue and the scaffold (Fig. 4A, arrows). Also notice the large nerve bundle alongside the muscle tissue (arrowheads). Large functional blood vessels were discernible in the TE muscle constructs, as indicated by the erythrocytes and the association of pericytes with the vessels (Fig. 4B). According to the previous finding that tissues engineered with both MPCs and ECs contained more blood vessels, we hypothesized that such an increase in vasculature would result in a corresponding increase in engineered muscle formation. Quantitative surface analysis of the TE muscle constructs (as shown in Fig. 4A) indicated that scaffolds seeded with both MPCs and ECs had significantly more tissue per HPF than scaffolds seeded with MPCs alone (Fig. 4C).

After observing an increased presence of vasculature and greater formation of tissue in dual MPC/EC seeded scaffolds, we wanted to determine if the muscle fibers generated from the seeded scaffolds were potentially functional. To do so, as an indirect indication of the force-producing capability of the TE muscle, the expression and localization of proteins known to be involved in the contraction process were analyzed. Simplistically, the development of functional skeletal muscle requires the formation of (1) a highly organized arrangement of force-bearing (i.e., generating and transmitting) proteins, (2) triadic structures (i.e., a close spatial arrangement of transverse tubules with terminal cisternae of the sarcoplasmic reticulum), and (3) neuromuscular junctions [16–18]. Desmin is an intermediate filament protein that plays an important role in the maintenance of myofibril organization and the transmission of forces generated during myosine–actin interactions [19]. Proper desmin localization was found in the TE muscle constructs, suggesting correct arrangement of the sarcomeres (Fig. 5A). Moreover, the heavy chain subunit of myosin (MyHC) has several isoforms that are sequentially expressed during development [20]. Using antibodies specific to neonatal (NMyHC) or adult (AMyHC) isoforms of MyHC, we were able to show that only the AMyHC isoform was expressed in the TE muscle constructs, with no expression of NMyHC detected (Fig. 5C,D). In addition to the expression of organized sarcomeric proteins, muscle contraction is dependent on the sarcoplasmic reticulum calcium release upon membrane depolarization (i.e., excitation-contraction coupling) and re-uptake [18]. Ryanodine receptor-1 (RyR1) [21] and junctophilin-1 (JP1) [22], proteins crucial for excitation-contraction coupling, were also expressed and properly localized along muscle fibers in a striated manner further supporting the potential contractile capability of the TE muscle (Fig. 5E,F). Lastly, the ability to self-regenerate is a vital property of mature myofibers, and is by and large carried out by Pax7-expressing resident satellite cells [23,24]. As seen in Fig. 5B, the TE muscle constructs revealed many $Pax7^{+}$ nuclei, which were localized under the basal lamina of the myofibers [23], further suggesting normal regeneration and maturity of the TE muscle.

Finally, the innervation of the TE muscle constructs was examined in order to further demonstrate the generation of myofibers with contractile potential. Nerve bundles were found adjacent to, and inter-mixed with the TE muscle fibers (Fig. 6A). In addition, neurovascular bundles, such as those found in functional muscle tissue, were found closely associated with the TE muscle (Fig. 6B, arrows and stars). Quantitative analyzes of βIII tubulin labeled nerve bundles showed a trend toward an increased number of nerves present in TE muscle constructs derived from scaffolds seeded with MPCs and ECs, compared with scaffolds seeded with MPCs only (Fig. 6C).

3.3. Real-time fluorescent microscopy to examine the growth and differentiation of TE muscle *in vitro*

In the previous examinations, we demonstrated that co-seeding of ECs with MPCs on a BAM scaffold resulted in increased vascularization and innervation of TE muscle *in vivo*. Furthermore, we demonstrated the utility of using fluorescent labels for tracking the location and organization of the implanted cells. To further explore optimal techniques for the engineering of muscle tissues, we added pericytes (PCs) to the culture of MPCs and ECs. PCs play an important role in blood vessel maturation and stabilization, and consequently, the formation of functional vascularized muscle tissue [25–27]. Qtracker705 was chosen as the fluorescent label for PCs since the emission range of this fluorophore is distinct from that of GFP and CM-DiI. In order to test the ability to simultaneously track cells labeled with the different fluorophores, the 3 cell types (MPCs, ECs, PCs) were co-seeded *in vitro* on matrigel, and cellular organization was imaged using fluorescent microscopy. CM-DiI labeled ECs assembled into capillary-like structures that were closely associated with PCs (Fig. 7A), as has been previously described [25]. When MPCs were added to the culture, each fluorophore was easily distinguished by fluorescent microscopy. Confocal microscopy was used to demonstrate 3-dimensional assembly of vessel-like structures formed by the ECs (Fig. 7B), as indicated by the presence of a lumen within the vessel (Fig. 7B, inset). When all cells were cultured on BAM in growth media (GM, described in “Methods”), ECs formed capillary-like structures that were associated with PCs in the presence of undifferentiated MPCs (Fig. 7C). The different cells were plainly distinguished by their fluorophores, which allowed for further imaging in real-time by fluorescent microscopy. When the seeded scaffolds were switched to differentiation media (DM) in culture, MPCs assembled into myotubes, which were associated with ECs and PCs (Fig. 7D). Live cell images of scaffolds, taken over time, show that the presence of PCs in the co-culture enhanced EC survival and growth (Fig. 7E). ImageJ software was used to quantitate the total DiI (+) pixels per HPF.

The ability to monitor cellular interactions in real time, while cells are grown on a scaffold, opens up the opportunity to dynamically test the effects of different growth modulating agents (e.g. biological and pharmacological agents) on cellular organization *in vitro*. As a proof-of concept, we utilized MPCs, ECs and PCs, in the previously described co-culture system, to examine the effect of VEGF on the formation and stabilization of capillary-like structures. Fluorescent imaging of cell seeded scaffolds, over time, showed an increased number of the branching vessel-like structures, in the presence of VEGF (Fig. 8A,B). Repetitive imaging of the same scaffold, over several days, allowed us to quantify the

stability of these branching vascular structures over time (Fig. 8C). The novelty of this finding lies in our ability to track and dynamically quantitate the effect of a biological factor on the organization of regenerating tissue structures. This data demonstrates the utility of this labeling procedure to identify and follow biological events in real-time and its further potential use as a screening platform for agents that effect the differentiation and tissue regenerative processes.

4. Discussion

The ability to engineer functional skeletal muscle is critically important for the restoration of quality of life to patients suffering from musculoskeletal defects, whether due to injury, aging or disease. The coordinated development of a functional vascular network, along with the growth of tissue engineered skeletal muscle, is essential in order to obtain sufficient tissue for clinical applications to the most devastating traumatic injuries. Furthermore, these technologies may be able to increase the rate and magnitude of recovery, ultimately hastening the recovery of motility. The purpose of this study was twofold: (1) to investigate the potential role of vascular cells in skeletal muscle tissue engineering, and (2) to explore fluorescent cell labeling as a means to track the interactions between different cell types and tissue organization in real time. Our data showed that incorporation of ECs, together with MPCs, for muscle TE enhanced vascularization, muscle tissue formation and innervation, in an *in vivo* model of subcutaneous implantation in nude mice. Furthermore, by using fluorescent cell labeling, we were able to track 2 cell types during the organization and differentiation of the TE muscle constructs *in vivo* and 3 cell types *in vitro*. These results are especially important for the evaluation of TE as a viable clinical approach to treat patients suffering from a wider range of severe muscle injuries.

In this study, we characterized the contribution of ECs to skeletal muscle tissue regeneration in a non-myogenic environment, using subcutaneous implantation in mice. Rodents have a remarkable ability for self-regeneration and healing that can mask the effect of implanted cells in the regenerative process. However, the use of the subcutaneous space model allowed us to determine the ability of exogenous MPCs to form muscle, while diminishing the confounding host regenerative effects. Our data demonstrated the ability of the implanted MPCs to form mature striated muscle fibers and that the addition of ECs enhanced vascularization, innervation and muscle tissue formation.

Incorporation of a functional vascular network is a requirement for functional regeneration of any tissue. The effect of vascular endothelial growth factor (VEGF) on angiogenesis after injury is well known. Recent publications have shown that MPCs secrete VEGF after injury resulting in new capillary formation, and reciprocally, VEGF secretion by ECs results in MPC migration and protection from apoptosis [28,29]. Several groups have recently shown that VEGF depletion in skeletal muscle results in a decrease number of myofiber associated capillaries [29]. *In vitro* data suggests that the simultaneous co-stimulation of MPCs and capillary formation is due to paracrine effects of VEGF as well as IGF-1, HGF, bFGF and PDGF-BB [30,31]. In contrast, it appears that the PCs associated with stable vessels secrete factors that inhibit myogenic growth and differentiation through the expression of Ang-1 and it's receptor Tie2 [32]. Our data demonstrated increased vascularization and tissue

growth on scaffolds seeded with both MPCs and ECs, which further confirms these results, and reinforces the need for concurrent vascularization during skeletal muscle tissue engineering.

Our data indicated increased innervation of TE muscle tissue on scaffolds that had been seeded with MPCs and ECs, and correspondingly, increased vascularization (Fig. 6). Secretion of VEGF by ECs is known to promote proliferation and migration of neural cells as well as aid in neurogenesis and provide neuro-protection [33,34]. In a reciprocal manner, secreted nerve factors affect angiogenesis by enhancing EC survival, vessel branching and vessel stabilization [35–37]. Therefore, it can be hypothesized that an increase in secretion of local VEGF due to increased vasculature would provide chemotactic cues resulting in increased migration of neurons into the muscle construct.

An effective means of promoting angiogenesis within a regenerating tissue has yet to be found. To this end, several strategies have been used in an attempt to enhance vascularization in TE muscle. The first method utilizes bioengineered scaffolds that have been designed to incorporate “channels” for the supply of nutrients to the regenerating tissue [38,39]. In a second approach, angiogenic growth factors are linked to a scaffold in order to entice the infiltration of host ECs into the regenerating tissue [40,41]. This approach has been largely ineffective due to the short half-life of most angiogenic growth factors. A third approach, and the approach that we employed, utilizes angiogenic cells and/or growth factors cultured with MPCs [42].

Several attempts have recently been made to enhance angio-genesis and vasculogenesis in order to establish a functional vascular network within regenerating skeletal muscle. In a recent study by Koffler *et al*., MPCs, ECs and fibroblasts were seeded on a biological acellular scaffold, similar to BAM, and implanted into an abdominal wall defect in nude mice [43]. Their data showed that the presence of ECs resulted in increased vasculature within developing myofibers after 3 weeks, whereas we demonstrate the survival and maintenance of TE vascularized muscles for up to 8 weeks after implantation. Moreover, the existence of vessels within our TE muscle constructs, made up from a mixture of implanted and host ECs, together with the presence of erythrocytes within these vessels, are consistent with the presence of a functional vascular network fully integrated with the host vascular system. This network of vessels is, in part, the result of a vasculogenic process and the formation of “chimeric” vessels, which is dependent on host vessel infiltration into the TE muscle and recruitment of implanted ECs.

The current study builds upon our recently published data demonstrating the ability of MPCs grown on BAM to differentiate into mature myofibers and contribute to functional restoration in a latissimus dorsi (LD) muscle deficit model [13,44]. These data show the contractile ability of TE muscle constructs on this scaffold and provides further evidence that our constructs may also be functional. Our current study suggested that the addition of ECs may further increase muscle volume and functional recovery after volumetric muscle loss in this model. Additionally, a recent publication by Corona *et al*. investigated the role of preconditioning on the ability of MPCs to form TE muscle on BAM and found that mechanical stretch via bioreactor preconditioning, as well as multiple cycles of cell seeding,

resulted in increased functional recovery in the same LD muscle deficit model [44]. This may explain our finding that all explanted scaffolds contained a mixture of aligned and disorganized fibers, which may have resulted from MPC differentiation in a non-native micro-environment, lacking in the mechanical strain that is customarily part of the typical skeletal muscle niche. Other studies have also confirmed that muscle alignment is partially dependent on mechanical stretch [45,46].

Finally, our data demonstrated the possibility of using fluorescently labeled cells for monitoring the growth, differentiation and tissue organization *in vivo* and *in vitro*. Currently the TE field is lacking the ability to monitor regeneration processes such as vascularization and maturation *in vivo* and in real time. Current imaging modalities either have the ability to monitor tissue in real time at low resolution (CT, MRI, PET) or require the sacrifice of the sample for high resolution imaging (i.e. microscopy). We recently published a study that demonstrated the development of a novel imaging system utilizing miniature fiber optical devices for nondestructive, single-cell-level resolution imaging of bioengineered tissue constructs [47,48]. The current study demonstrates the ability to positively identify implanted GFP-MPCs and -ECs after 8 weeks implantation *in vivo*, a sufficiently long enough time to follow many regenerative processes. In ethese experiments we showed the ECs, which were labeled via a non-genetic labeling method (the cell dye CM-Di, retained strong enough signal to be detected after 2 months *in vivo*. Subsequently, we demonstrated the ability to image the interactions and differentiation capabilities of 3 fluorescently labeled cell types: MPCs, ECs and PCs, in real time *in vitro*, demonstrating a biological fluorescent imaging application. Combining the method developed here with the fiber-optic-based imaging modality described before [47,48], it will be possible to document tissue development and monitor the dynamic interplay between multiple cells types *in vivo*, in real-time, and with single-cell-level resolution. Such a technology may serve as a potent platform for testing the effects of different biological or pharmacological agents on tissue regeneration.

5. Conclusions

Combination of ECs and MPCs, seeded together on ECM scaffolds and implanted *in vivo*, induced more vascularization, tissue formation and innervation than scaffolds seeded with MPCs alone. The use of the subcutaneous space model of *in vivo* muscle development allowed us to examine the maturation of the implanted TE muscle constructs without confounding host effects. The TE muscle contained fully mature myofibers that showed appropriate expression and localization of several protein markers involved in contraction, suggesting the potential functionality of these constructs. Fluorescent cell labeling allowed for the examination of the interactions and differentiation capabilities of MPCs, EPCs and PCs grown on the BAM scaffold *in vitro* in real time.

Supplementary Material

Refer to Web version on PubMed Central for supplementary material.

Acknowledgments

This work was supported by the U.S. Department of Defense Armed Forces Institute of Regenerative Medicine (USAMRAA AFIRM W81XWH-08-2-0032 to S.S). The neonatal myosin heavy chain, Pax7 and RyR antibodies (developed by E. Bandman, A. Kawakami, J. Airey and J. Sutko respectively) were obtained from the Developmental Studies Hybridoma Bank developed under the auspices of the National Institute of Child Health and Human Development and maintained by the University of Iowa, Department of Biology (Iowa City, IA).

References

1. Atala A. Regenerative medicine strategies. J Pediatr Surg. 2012; 47:17–28. [PubMed: 22244387]
2. Badylak SF, Weiss DJ, Caplan A, Macchiarini P. Engineered whole organs and complex tissues. Lancet. 2012; 379:943–52. [PubMed: 22405797]
3. Krawiec JT, Vorp DA. Adult stem cell-based tissue engineered blood vessels: a review. Biomaterials. 2012; 33:3388–400. [PubMed: 22306022]
4. Kusuma S, Gerecht S. Engineering blood vessels using stem cells: innovative approaches to treat vascular disorders. Expert Rev Cardiovasc Ther. 2010; 8:1433–45. [PubMed: 20936930]
5. Borschel GH, Dennis RG, Kuzon WM Jr. Contractile skeletal muscle tissue-engineered on an acellular scaffold. Plast Reconstr Surg. 2004; 113:595–602. discussion 3–4. [PubMed: 14758222]
6. De Coppi P, Bellini S, Conconi MT, Sabatti M, Simonato E, Gamba PG, et al. Myoblast-acellular skeletal muscle matrix constructs guarantee a long-term repair of experimental full-thickness abdominal wall defects. Tissue Eng. 2006; 12:1929–36. [PubMed: 16889522]
7. Levenberg S, Rouwkema J, Macdonald M, Garfein ES, Kohane DS, Darland DC, et al. Engineering vascularized skeletal muscle tissue. Nat Biotechnol. 2005; 23:879–84. [PubMed: 15965465]
8. Nomi M, Miyake H, Sugita Y, Fujisawa M, Soker S. Role of growth factors and endothelial cells in therapeutic angiogenesis and tissue engineering. Curr Stem Cell Res Ther. 2006; 1:333–43. [PubMed: 18220878]
9. De Coppi P, Delo D, Farrugia L, Udompanyanan K, Yoo JJ, Nomi M, et al. Angiogenic gene-modified muscle cells for enhancement of tissue formation. Tissue Eng. 2005; 11:1034–44. [PubMed: 16144439]
10. Saik JE, Gould DJ, Watkins EM, Dickinson ME, West JL. Covalently immobilized platelet-derived growth factor-BB promotes angiogenesis in biomimetic poly(ethylene glycol) hydrogels. Acta Biomater. 2011; 7:133–43. [PubMed: 20801242]
11. Delo DM, Eberli D, Williams JK, Andersson KE, Atala A, Soker S. Angiogenic gene modification of skeletal muscle cells to compensate for ageing-induced decline in bioengineered functional muscle tissue. BJU Int. 2008; 102:878–84. [PubMed: 18489526]
12. Lang I, Schweizer A, Hiden U, Ghaffari-Tabrizi N, Hagendorfer G, Bilban M, et al. Human fetal placental endothelial cells have a mature arterial and a juvenile venous phenotype with adipogenic and osteogenic differentiation potential. Differentiation. 2008; 76:1031–43. [PubMed: 18673379]
13. Machingal MA, Corona BT, Walters TJ, Kesireddy V, Koval CN, Dannahower A, et al. A tissue-engineered muscle repair construct for functional restoration of an irrecoverable muscle injury in a murine model. Tissue Eng Part A. 2011; 17:2291–303. [PubMed: 21548710]
14. Criswell TL, Corona BT, Ward CL, Miller M, Patel M, Wang Z, et al. Compression-induced muscle injury in rats that mimics compartment syndrome in humans. Am J Pathol. 2012; 180:787–97. [PubMed: 22133601]
15. Schmalbruch H. The morphology of regeneration of skeletal muscles in the rat. Tissue Cell. 1976; 8:673–92. [PubMed: 1020021]
16. Clark KA, McElhinny AS, Beckerle MC, Gregorio CC. Striated muscle cytoarchitecture: an intricate web of form and function. Ann Rev Cell Dev Biol. 2002; 18:637–706. [PubMed: 12142273]
17. Kaariainen M, Ka Duhanen S. Skeletal muscle injury and repair: the effect of disuse and denervation on muscle and clinical relevance in pedicled and free muscle flaps. J Reconstr Microsurg. 2012

18. Lee EH. Ca2+ channels and skeletal muscle diseases. Prog Biophys Mol Biol. 2010; 103:35–43. [PubMed: 20553745]
19. Sam M, Shah S, Friden J, Milner DJ, Capetanaki Y, Lieber RL. Desmin knockout muscles generate lower stress and are less vulnerable to injury compared with wild-type muscles. Am J Physiol Cell Physiol. 2000; 279:C1116–22. [PubMed: 11003592]
20. Schiaffino S, Reggiani C. Fiber types in mammalian skeletal muscles. Physiol Rev. 2011; 91:1447–531. [PubMed: 22013216]
21. Capes EM, Loaiza R, Valdivia HH. Ryanodine receptors. Skelet Muscle. 2011; 1:18. [PubMed: 21798098]
22. Golini L, Chouabe C, Berthier C, Cusimano V, Fornaro M, Bonvallet R, et al. Junctophilin 1 and 2 proteins interact with the L-type Ca2+ channel dihydropyridine receptors (DHPRs) in skeletal muscle. J Biol Chem. 2011; 286:43717–25. [PubMed: 22020936]
23. Cossu G, Biressi S. Satellite cells, myoblasts and other occasional myogenic progenitors: possible origin, phenotypic features and role in muscle regeneration. Semin Cell Dev Biol. 2005; 16:623–31. [PubMed: 16118057]
24. Jarvinen TA, Jarvinen TL, Kaariainen M, Kalimo H, Jarvinen M. Muscle injuries: biology and treatment. Am J Sports Med. 2005; 33:745–64. [PubMed: 15851777]
25. Egginton S, Hudlicka O, Brown MD, Graciotti L, Granata AL. In vivo pericyteendothelial cell interaction during angiogenesis in adult cardiac and skeletal muscle. Microvasc Res. 1996; 51:213–28. [PubMed: 8778576]
26. Egginton S, Zhou AL, Brown MD, Hudlicka O. The role of pericytes in controlling angiogenesis in vivo. Adv Exp Med Biol. 2000; 476:81–99. [PubMed: 10949657]
27. Zembron-Lacny A, Krzywanski J, Ostapiuk-Karolczuk J, Kasperska A. Cell and molecular mechanisms of regeneration and reorganization of skeletal muscles. Ortop Traumatol Rehabil. 2012; 14:1–11. [PubMed: 22388356]
28. Germani A, Di Carlo A, Mangoni A, Straino S, Giacinti C, Turrini P, et al. Vascular endothelial growth factor modulates skeletal myoblast function. Am J Pathol. 2003; 163:1417–28. [PubMed: 14507649]
29. Ochoa O, Sun D, Reyes-Reyna SM, Waite LL, Michalek JE, McManus LM, et al. Delayed angiogenesis and VEGF production in CCR2-/- mice during impaired skeletal muscle regeneration. Am J Physiol Regul Integr Comp Physiol. 2007; 293:R651–61. [PubMed: 17522124]
30. Doukas J, Blease K, Craig D, Ma C, Chandler LA, Sosnowski BA, et al. Delivery of FGF genes to wound repair cells enhances arteriogenesis and myogenesis in skeletal muscle. Mol Ther. 2002; 5:517–27. [PubMed: 11991742]
31. Walgenbach KJ, Gratas C, Shestak KC, Becker D. Ischaemia-induced expression of bFGF in normal skeletal muscle: a potential paracrine mechanism for mediating angiogenesis in ischaemic skeletal muscle. Nat Med. 1995; 1:453–9. [PubMed: 7585094]
32. Abou-Khalil R, Mounier R, Chazaud B. Regulation of myogenic stem cell behavior by vessel cells: the “menage a trois” of satellite cells, periendothelial cells and endothelial cells. Cell Cycle. 2010; 9:892–6. [PubMed: 20160472]
33. Jin K, Zhu Y, Sun Y, Mao XO, Xie L, Greenberg DA. Vascular endothelial growth factor (VEGF) stimulates neurogenesis in vitro and in vivo. Proc Natl Acad Sci U S A. 2002; 99:11946–50. [PubMed: 12181492]
34. Ruiz de Almodovar C, Fabre PJ, Knevels E, Coulon C, Segura I, Haddick PC, et al. VEGF mediates commissural axon chemoattraction through its receptor Flk1. Neuron. 2011; 70:966–78. [PubMed: 21658588]
35. Calza L, Giardino L, Giuliani A, Aloe L, Levi-Montalcini R. Nerve growth factor control of neuronal expression of angiogenetic and vasoactive factors. Proc Natl Acad Sci U S A. 2001; 98:4160–5. [PubMed: 11259645]
36. Donovan MJ, Lin MI, Wiegn P, Ringstedt T, Kraemer R, Hahn R, et al. Brain derived neurotrophic factor is an endothelial cell survival factor required for intramyocardial vessel stabilization. Development. 2000; 127:4531–40. [PubMed: 11023857]

37. Mukouyama YS, Shin D, Britsch S, Taniguchi M, Anderson DJ. Sensory nerves determine the pattern of arterial differentiation and blood vessel branching in the skin. Cell. 2002; 109:693–705. [PubMed: 12086669]
38. Cui X, Boland T. Human microvasculature fabrication using thermal inkjet printing technology. Biomaterials. 2009; 30:6221–7. [PubMed: 19695697]
39. Nalayanda DD, Wang Q, Fulton WB, Wang TH, Abdullah F. Engineering an artificial alveolar-capillary membrane: a novel continuously perfused model within microchannels. J Pediatr Surg. 2010; 45:45–51. [PubMed: 20105578]
40. Odedra D, Chiu LL, Shoichet M, Radisic M. Endothelial cells guided by immobilized gradients of vascular endothelial growth factor on porous collagen scaffolds. Acta Biomater. 2011; 7:3027–35. [PubMed: 21601017]
41. Rahman N, Purpura KA, Wylie RG, Zandstra PW, Shoichet MS. The use of vascular endothelial growth factor functionalized agarose to guide pluripotent stem cell aggregates toward blood progenitor cells. Biomaterials. 2010; 31:8262–70. [PubMed: 20684984]
42. Wang Z, He Y, Yu X, Fu W, Wang W, Huang H. Rapid vascularization of tissue-engineered vascular grafts in vivo by endothelial cells in co-culture with smooth muscle cells. J Mater Sci Mater Med. 2012; 23:1109–17. [PubMed: 22331376]
43. Koffler J, Kaufman-Francis K, Shandalov Y, Egozi D, Pavlov DA, Landesberg A, et al. Improved vascular organization enhances functional integration of engineered skeletal muscle grafts. Proc Natl Acad Sci U S A. 2011; 108:14789–94. [PubMed: 21878567]
44. Corona BT, Machingal MA, Criswell T, Vadhavkar M, Dannahower AC, Bergman C, et al. Further development of a tissue engineered muscle repair construct in vitro for enhanced functional recovery following implantation in vivo in a murine model of volumetric muscle loss injury. Tissue Eng Part A. 2012; 18:1213–28. [PubMed: 22439962]
45. Haghighipour N, Heidarian S, Shokrgozar MA, Amirizadeh N. Differential effects of cyclic uniaxial stretch on human mesenchymal stem cell into skeletal muscle cell. Cell Biol Int. 2012; 36:669–75. [PubMed: 22681392]
46. Hicks MR, Cao TV, Campbell DH, Standley PR. Mechanical strain applied to human fibroblasts differentially regulates skeletal myoblast differentiation. J Appl Physiol. 2012
47. Hofmann MC, Whited BM, Criswell T, Rylander MN, Rylander CG, Soker S, et al. A fiber-optic-based imaging system for nondestructive assessment of cell-seeded tissue-engineered scaffolds. Tissue Eng Part C Methods. 2012
48. Hofmann MC, Whited BM, Mitchell J, Vogt WC, Criswell T, Rylander C, et al. Scanning-fiber-based imaging method for tissue engineering. J Biomed Opt. 2012; 17:066010. [PubMed: 22734766]

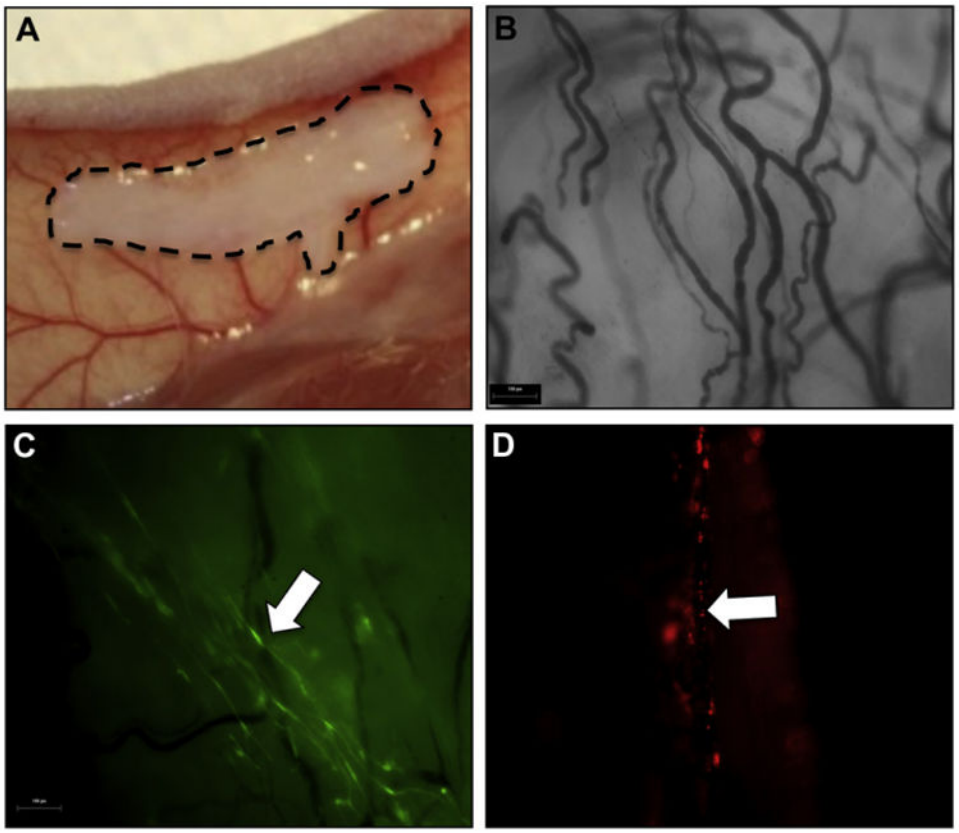

Fig. 1.

Gross morphology of TE muscle upon explantation. Gross morphology of cell-seeded BAM scaffolds after explantation from the subcutaneous space of nude mice, 8 weeks post implantation. (A) Location of implanted scaffold in the mid-dorsal subcutaneous space. Hatched marks outline the scaffold. (B) Bright field microscopy showed branching vascular network throughout the construct. (C, D) Fluorescent MPCs (C, green) and ECs (D, red) are visible in the scaffold, through the use of fluorescent microscopy. Arrows indicate elongated GFP + MPCs (C) and ECs integrated into the vasculature (D). Scale bars: 100 μm. (For interpretation of the references to colour in this figure legend, the reader is referred to the web version of this article.)

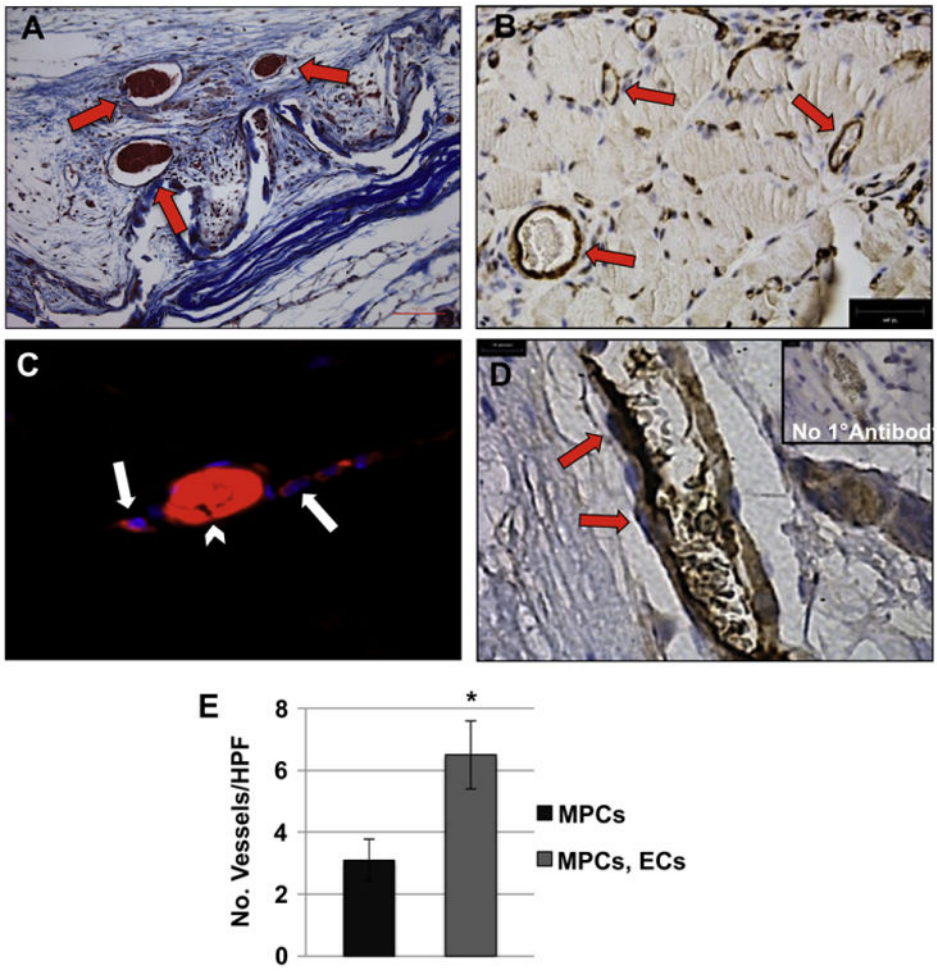

Fig. 2.

Integration of implanted ECs in the TE muscle vasculature. (A) Masson's trichrome stain demonstrated the presence of blood vessels within the scaffold (arrows). The collagen scaffold is stained light blue. Scale bar: 200 μm. (B) Immunohistochemistry for CD146 showed pericyte-covered blood vessels (arrows) distributed within the engineered muscle tissue. (C) Fluorescent microscopy showed integration of DiI-labeled ECs (red, arrow) into a blood vessel containing erythrocytes (autofluorescence in red, arrow-head). (D) The identity of implanted human ECs was confirmed using a human-specific anti-CD31 antibody (arrows, positive CD31 staining). Inset: control staining without primary antibody. (E) Blood vessels were quantified in constructs seeded with MPCs only to those dual seeded with MPCs and ECs, by counting the number of vessels visibly containing erythrocytes from ≥20 random trichrome stained HPFs. Data are expressed as means ± SEM for number of HPFs. Scale bars: 200 μm (A), 10 μm, (BeD). *$P < 0.04$. (For interpretation of the references to colour in this figure legend, the reader is referred to the web version of this article.)

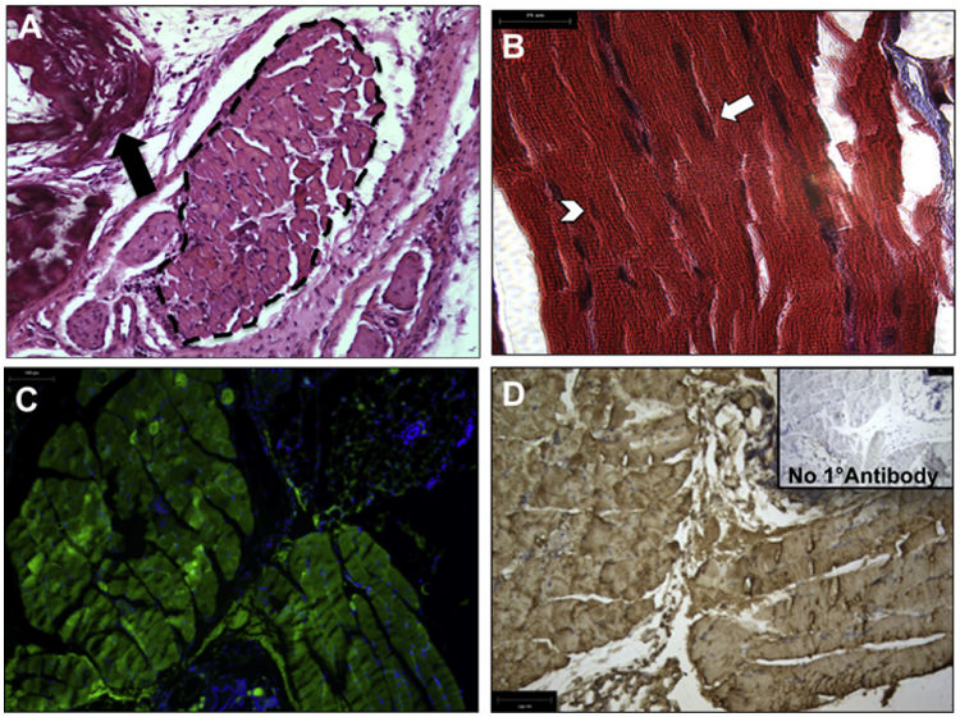

Fig. 3.

Implanted MPCs form organized muscle tissue *in vivo*. H + E (A) and Masson's trichrome stain (B) indicated the formation of myofibers on the explanted constructs. (A) Arrow indicates location of the scaffold. Hatched marks outline the muscle tissue. (B) Arrows indicate mature myofibers and arrowheads indicate immature myofibers, differentiated by the presence of peripherally and centrally located nuclei, respectively. Scale bars: 100 μm (C, D) Implanted GFP^+ MPCs form mature myofibers on the scaffold, as seen by fluorescence microscopy of GFP^+ myofibers (C) and IHC using anti-GFP antibodies. Inset, control staining without primary antibody. Scale bars: 50 μm.

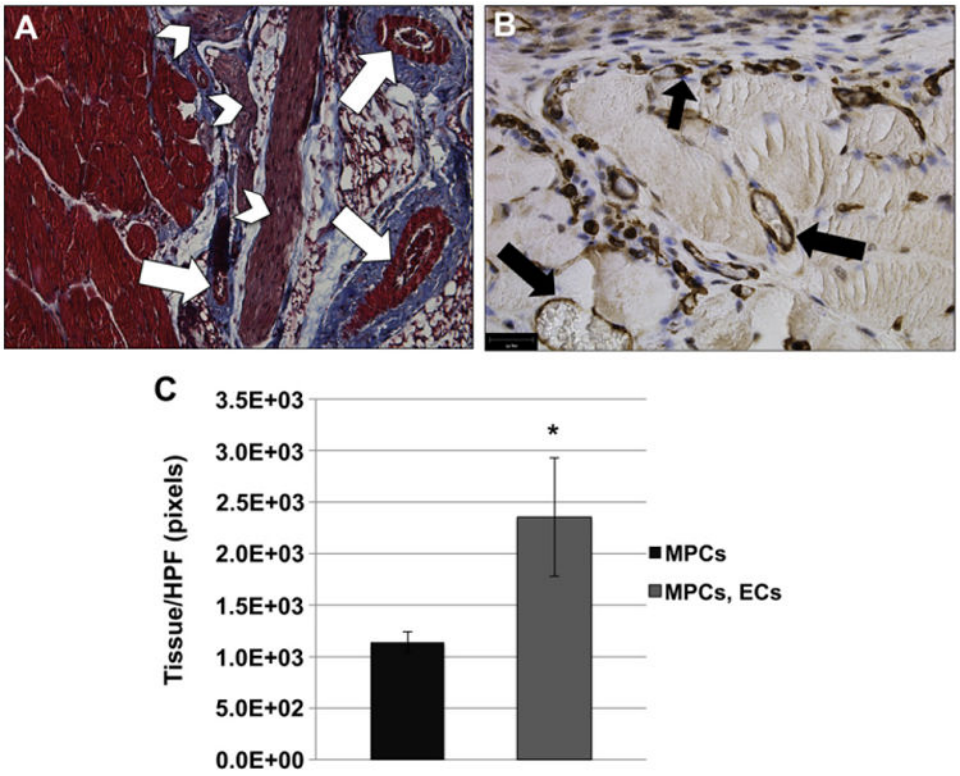

Fig. 4.

Combination of ECs, together with MPCs, improves muscle tissue formation *in vivo*. (A) Masson's trichrome stain was used to demonstrate the formation of muscle tissue (red) on the BAM scaffold. Arrows indicate blood vessels within the muscle tissue. Arrowheads indicate nerve bundles. Scale bar: 100 μm (B) CD146 IHC was used to demonstrate the presence of blood vessels localized within the muscle tissue (black arrows). Many small capillary-like vessels were found associated with the myofibers. Scale bar: 50 μm. (C) The amount of tissue was quantitated from ≥10 random trichrome stained HPFs using ImageJ analysis software. The data showed an increase in tissue area when scaffolds were seeded with both ECs and MPCs. Data are expressed as means ± SEM for number of HPFs. **P* < 0.03. (For interpretation of the references to colour in this figure legend, the reader is referred to the web version of this article.)

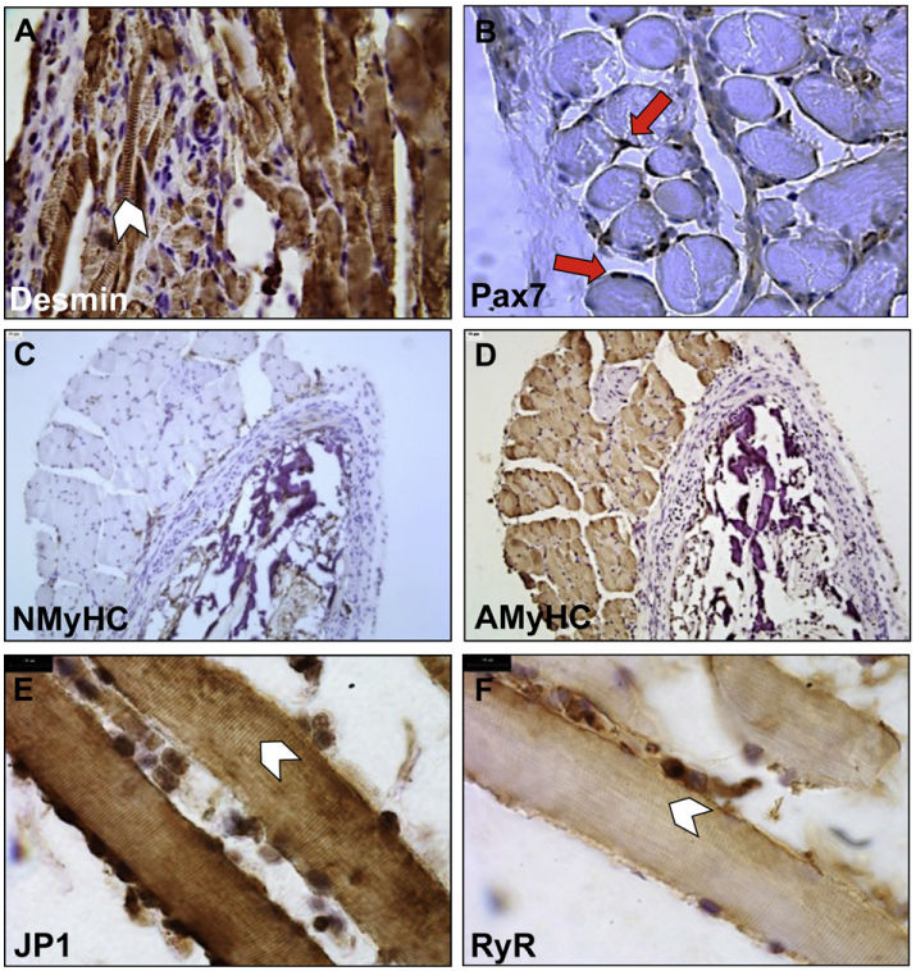

Fig. 5. Characterization of muscle markers in explanted TE muscle

TE muscle constructs were assessed by IHC for differentiation and functional muscle markers. Myofibers stained positively for desmin (A), contained $Pax7^{+}$ nuclei (red arrows) (B), were negative for neonatal MyHC (C), positive for adult MyHC (D), positive for JP1 (E) and RyR1 (F). Desmin, JP1 and RyR1 were properly localized within the striated bands of the sarcomere (arrow-heads). Scale bars: 25 μm(A–D), 10 μm (E, F). (For interpretation of the references to colour in this figure legend, the reader is referred to the web version of this article.)

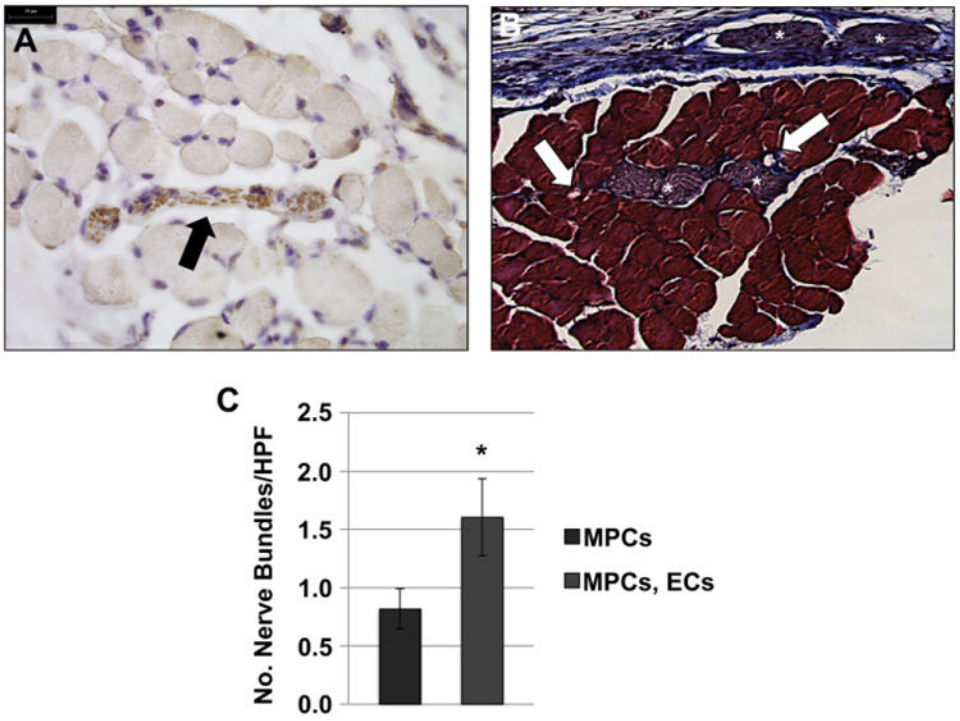

Fig. 6. Combination of ECs with MPCs improves muscle tissue innervation *in vivo*

(A) βIII tubulin staining indicated nerve bundles interspersed with the myofibers on the scaffolds. (B) Neuro-vascular bundles were observed in trichrome stained sections of explanted TE muscle constructs (asterisks - nerve bundles; arrows - blood vessels). Scale bars: 25 μm. (C) Quantification of βIII tubulin-positive nerve bundles in ≥20 random HPFs, showed a trend towards an increase of nerve bundle number when scaffolds were seeded with both ECs and MPCs. Data are expressed as means ± SEM for number of HPFs. *$P < 0.06$.

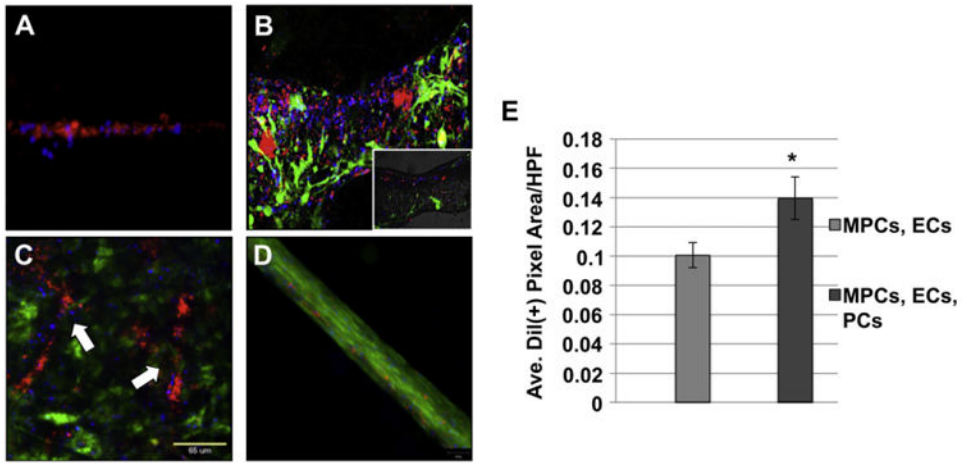

Fig. 7.

Fluorescent imaging of TE muscle *in vitro*. MPCs, ECs and PCs were co-cultured together on either Matrigel™-coated dishes (A, B) or on the BAM scaffold (C, D) and live cell imaging was performed using fluorescent microscopy. (A) PCs labeled with Qtracker705 (blue) are localized around the periphery of DiI-labeled ECs (red) vascular structures. (B) Confocal microscopy demonstrated a 3-dimensional image of vessels consisting of GFP^+ MPCs (green), DiI-labeled ECs (red) and PCs labeled with Qtracker 705 (blue). Inset shows the lumen of a blood vessel. Co-cultures of ECs, MPCs and PCs grown on BAM in either GM (C) or differentiated in DM (D) were visualized using live cell imaging. Arrows (C) indicate branched vessel-like structures. Scale bars: 65 μm (E) EC content on the BAM scaffold was determined by quantitating the amount of DiI^+ pixels from ≥30 random HPFs, and showed the presence of more ECs when co-cultured with MPCs and PCs, compared with ECs and MPCs only. Data are expressed as means ± SEM for number of HPFs. Experiment was performed in triplicate. $*P < 0.02$. (For interpretation of the references to colour in this figure legend, the reader is referred to the web version of this article.)

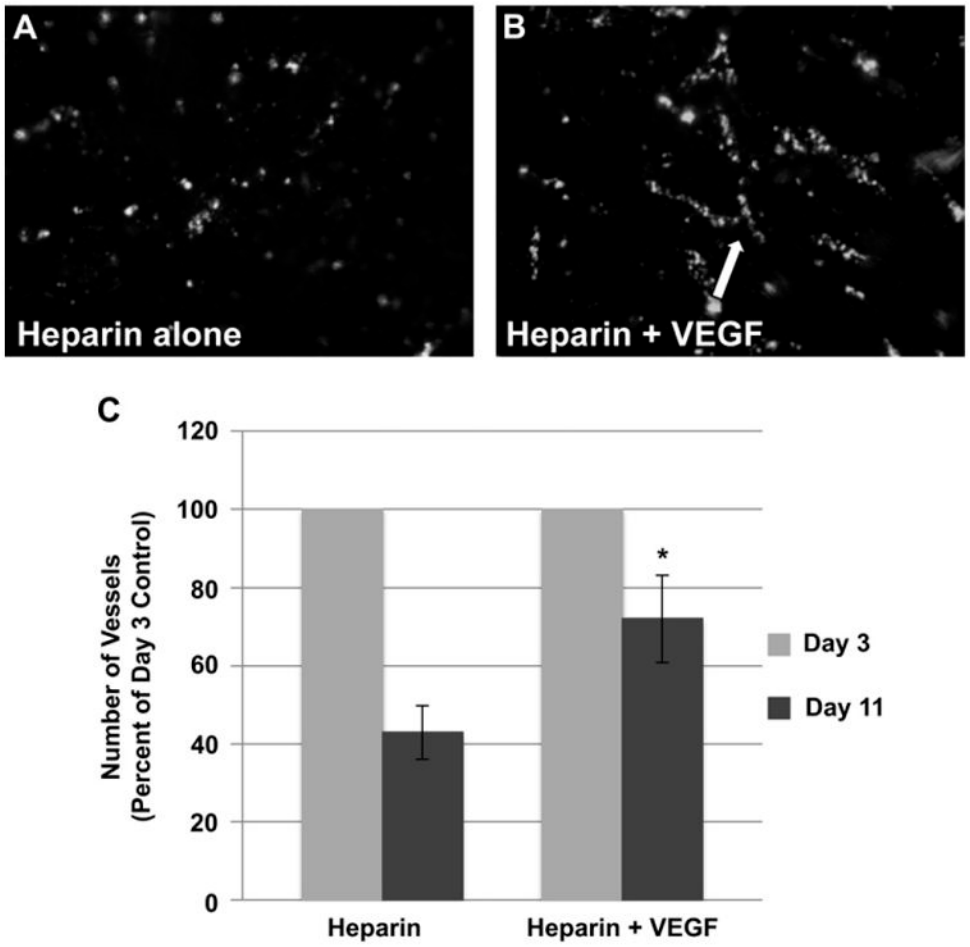

Fig. 8.

The effect of VEGF on the formation of vascular structures *in vitro*. Images of capillary-like structures formed by ECs, co-cultured with MPCs and PCs, in the absence (A) or presence (B) of VEGF. Arrow indicates branching of capillary-like structure. (C) The number of vascular structures was quantitated by counting the number of branches present on the scaffold over time. The number of branches counted from ≥30 random HPFs is higher on day 11 in the presence of VEGF. Data are expressed as means ± SEM for number of HPFs. Experiment was performed in triplicate. *$P < 0.02$.

Table 1

Antibody summary.

Primary antibodies (Dilution)	Secondary biotinylated antibodies (Dilution)	Company (Catalog number)
Human CD31 (1:50)	Mouse (1:500)	Dako (M0823)
CD146 (1:50)	Mouse (1:500)	Millipore (04–1147)
GFP (1:100)	Rabbit (1:500)	Abcam (ab290)
Desmin (1:75)	Mouse (1:500)	Dako (M0760)
βIII tubulin	Mouse (1:500)	Promega (G7121)
Adult MyHC (1:100)	Goat (1:500)	Santa Cruz (12117)
Neonatal MyHC (1:100)	Mouse (1:500)	Developmental Studies Hybridoma Bank (DSHB) (2E9)
RyR1 (1:50)	Mouse (1:500)	DSHB (34C-c)
JP1 (1:250)	Rabbit (1:500)	Invitrogen (405100)
Pax7 (1:100)	Mouse (1:500)	DSHB (Pax7)